The San Andreas Fault of the Salton Trough Region, California, as Expressed on Remote Sensing Data

FRANCESCO V. CORONA *Energy Resources Technology Division, P. O. Box 76 , Brea, California 92621*
FLOYD F. SABINS, JR. *Remote Sensing Enterprises, 1724 Celeste Lane, Fullerton, California 92633*

ABSTRACT

The San Andreas fault and related structures in the Salton trough region are readily expressed on Landsat images and high-altitude aerial photographs, having diagnostic surface characterisitics that are typical of a wrench-fault assemblage. These characteristics include a principal strike-slip displacement zone that is relatively straight and long, inconsistent structural relief along major wrench faults, the occurrence of en *echelon* structures adjacent to the major strike-slip faults, and lateral offset of structural, natural, and man-made features. Wrench-fault transpression and transtension occur in places along the San Andreas fault system, recognized respectively by the dominance of contractional or extensional structures. All of these surface manifestations are clearly discriminated on the remote sensing data and define criteria that distinguish wrench-fault assemblages from other structural styles.

INTRODUCTION

The southern extent of the San Andreas right-lateral, strike-slip fault lies along the northeastern margin of the Salton trough in southern California (Figure 1). This fault is tectonically active, well exposed, and well documented in this region (many authors; e.g., Crowell, 1962; Dibblee, 1977; Crowell and Sylvester, 1979; Sylvester, 1988; Hutton and others, 1991), thus offering an ideal locality to study the San Andreas fault and the structural assemblage that is commonly associated with wrench-fault tectonics (Figure 2; Wilcox and others, 1973; Harding, 1974; Reading, 1980; Christie-Blick and Biddle, 1985; Harding, 1990). Wrench-fault assemblages have unique structural characteristics that differentiate them from other styles of deformation (Harding and Lowell, 1979; Lowell, 1990). Likewise, wrench-fault assemblages have distinguishing surface manifestations that can be detected and analyzed using remote sensing data (Corona, 1993).

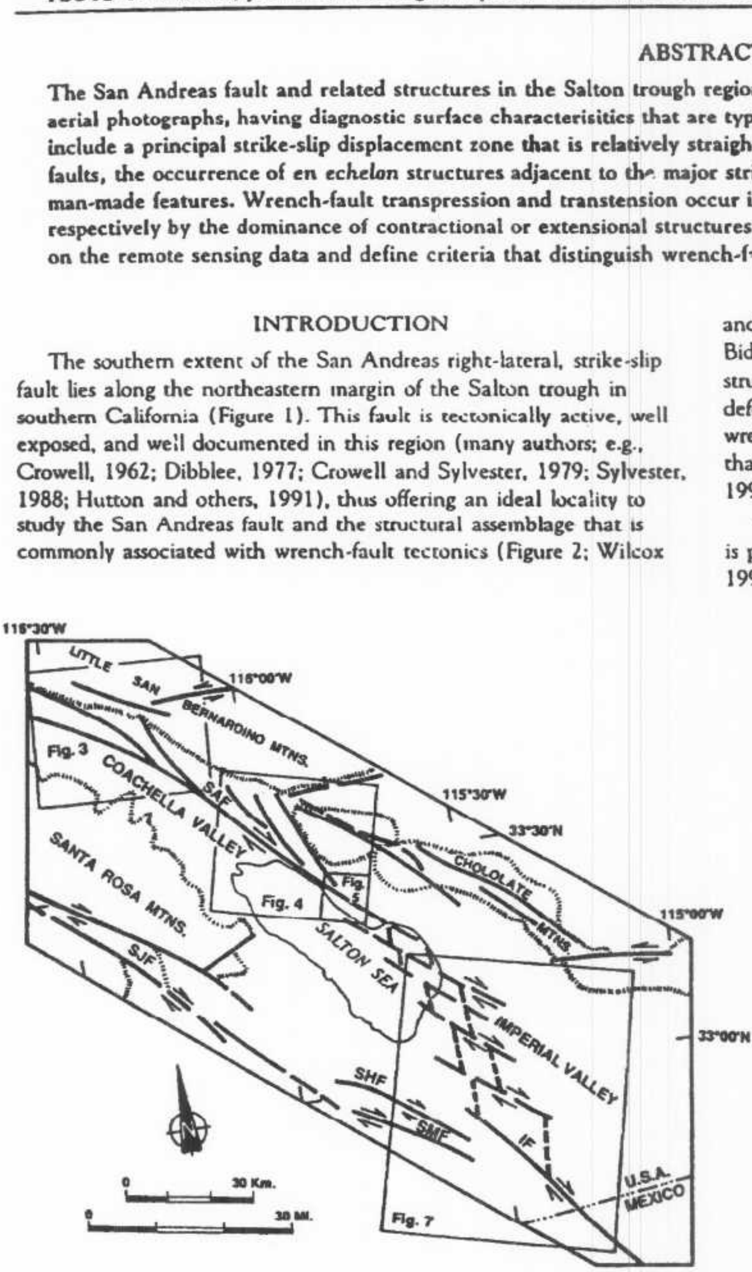

Figure 1. Location map of the Salton trough region of southern California showing the major strike-slip (wrench) fault systems and areas of investigation (Figures 3, 4, 5, and 7). These areas are, from northwest to southeast, the Indio Hills, the Mecca Hills, the Durmid Hills, and the Imperial Valley. IF, Imperial fault; SAF, San Andreas fault; SHF, Superstition Hills fault; SJF, San Jacinto fault; SMF, Superstition Mountain fault.

The San Andreas wrench-fault system in the Salton trough region is profoundly displayed on remote sensing data (Corona and others, 1993). Examination of this fault system using these data yields diagnostic surface characteristics that define criteria to distinguish a wrench-fault structural assemblage from other structural styles. The following discussion describes the identification criteria of wrench-fault assemblages from remote sensing data utilizing Landsat Thematic Mapper images and high-altitude aerial photographs along this Salton trough segment of the San Andreas fault system.

AREAS OF INVESTIGATION

Four areas along the San Andreas fault system in the Salton trough are selected to show the diagnostic surface characteristics of wrench-fault assemblages as expressed on remote sensing data (see Figure 1). These areas are the Indio, Mecca, and Durmid hills, and the Imperial Valley. The Indio Hills display classic neotectonic wrench-fault morphology, whereas the Mecca Hills reveal a suite of wrench-related structural elements. Wrench-fault transpression dominates the Durmid Hills, and transtension is prevalent in the Imperial Valley. These areas conjointly constitute most of the structural characteristics that typify a wrench-fault structural style. In turn, these structural characteristics provide the criteria for the identification of wrench-fault assemblages from remote sensing or any geologic-map data. The compilation of these criteria are summarized at the end of this discussion.

Indio Hills

The Indio Hills form a low northwest-trending ridge along the northeastern margins of the Coachella Valley and Salton trough (Figure 3). The uplift is 20 miles long, up to four miles wide, and rises to maximum elevations of 1600 to 1700 feet.

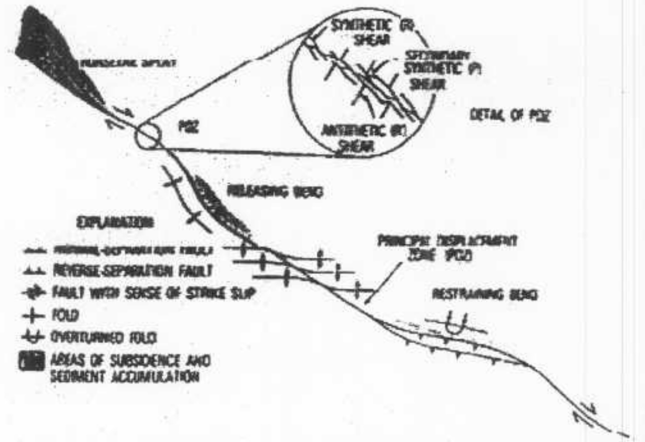

Figure 2. An idealized right-slip wrench fault in map view showing structural elements that are commonly associated with such a wrench-fault system (from Christie-Blick and Biddle, 1985).

An alluvial valley up to two miles wide separates the Indio Hills from the Little San Bernardino Mountains to the northeast, which consist of crystalline bedrock. The Indio Hills are bordered on the southwest by the Coachella Valley that is being developed into housing tracts, resorts, golf courses, and agriculture. The Landsat Thematic Mapper data shown in Figure 3 depict irrigated vegetation and palm trees as a dark signature, exposed rocks as gray tones, and windblown sand with sparse native vegetation (creosote bush, mesquite, tamarisk) as light gray to white.

The generalized stratigraphic section of the Indio Hills consists of Plio-Pleistocene nonmarine clastic strata that were deposited upon a basement of granitic rocks (Cretaceous) and associated crystalline rocks. These rocks are exposed in the Little San Bernardino Mountains and are the source of the granitic and metamorphic detritus in the Neogene strata. The ridge-and-slope topography of the Indio Hills is composed of moderately indurated conglomeratic sandstone and micaceous siltstone of the Pliocene Palm Spring formation (Sabins, 1967). This contrasts with the uniform slopes formed by the equivalent Canebrake Conglomerate and younger Ocotillo Conglomerate (Pleistocene). The Pliocene-age Imperial and Mecca formations that underlie the Palm Spring formation occur in a few small outcrops in the northern and southern portions of the Indio Hills, but are not recognizable on the satellite data.

The northwestern two-thirds of the Indio Hills are cut by the sub-parallel Mission Creek and Banning right-slip faults. These faults merge southeastward as the continuation of the San Andreas fault and form the southwestern boundary of the Indio Hills. To the northwest, one or both of the Banning and Mission Creek faults merge with the San Andreas fault, but the relationship is not clear. The Banning and Mission Creek faults are both active faults with numerous historic earthquakes.

The Mission Creek fault passes through the town of Desert Hot Springs and strikes southeastward through the valley for six miles to the northwestern end of the Indio Hills. For three miles southeast of Desert Hot Springs the northeastern side of the fault is marked by a row of low hills of older alluvium that are truncated on their southwestern flanks by linear fault scarps. These fault-controlled hills are obvious on the Landsat image (see Figure 3). Southeast from the

Figure 3. Landsat Thematic Mapper mosaic of the Indio Hills region, California. Large black arrows mark the three major right-slip faults that cut the uplift: from southwest to northeast, Banning, Mission Creek, and Indio faults. Small black arrows depict right-slip offset of canyons along the strike-slip faults, and open arrows point to where the strike-slip faults act as barriers to groundwater flow. eh, Edom Hill; dhs, Desert Hot Springs; tpc, Thousand Palms Canyon. Images were processed at Chevron Oil Field Research Company, La Habra, California.

Figure 4. Landsat Thematic Mapper image of the Mecca Hills area, California, showing the major structures associated with the San Andreas fault system. The Mecca Hills lie between the Coachella Valley and Orocopia Mountains. Image was processed at Unocal Remote Sensing Laboratory, Brea, California.

hills, the Mission Creek fault forms the northeastern margin of the Indio Hills. Note that the topographic and corresponding structural relief have shifted along the right-slip fault. Farther southeast, the Mission Creek fault crosses Thousand Palms Canyon where it forms a barrier to groundwater that results in springs and the Thousand Palms Oasis on the northeastern side of the fault. The oasis supports a dense grove of native palm trees. Southeast from Thousand Palms Canyon, the Mission Creek fault cuts diagonally through the Indio Hills and offsets the southwest-flowing canyons in a right-lateral sense.

The Banning fault strikes eastward along the northern margin of San Gorgonio Pass and curves southeastward across the northern end of Coachella Valley. The Banning fault separates Edom Hill on the south from the northern portion of the Indio Hills. Southeast from Edom Hill, the fault is the southern margin of the Indio Hills. Again, the structural and associated topographic highs have shifted along the strike-slip fault (see figure [illegible]). Five miles southeast of Thousand Palms Canyon, the Banning and Mission Creek faults merge and strike southeastward along the Indio Hills as the San Andreas fault.

The trace of the Banning fault is marked by a conspicuous linear tonal anomaly on the Landsat image (see Figure 3). The northeastern side of the fault has an anomalous dark signature with scattered patches of irrigated vegetation and some housing developments. To the southwest, the tone changes abruptly to the light-colored signature that is characteristic of the windblown sand that covers much of the northern Coachella Valley. Housing developments and irrigated vegetation are lacking in this barren region. The remarkably sharp linear contact between these contrasting Landsat signatures extends northwest along the Banning fault for four miles where it is concealed beneath windblown sand. The following explanation for this Landsat anomaly is based on field observations here and at similar anomalies along other faults in the region. In the northern Coachella Valley, the Banning fault is a barrier to the southward flow of groundwater. Along the northeastern side of the fault the water table is shallow which supports phreatophytes such as tamarisk, mesquite, and creosote bushes. This vegetation blocks the eastward migration of windblown sand; therefore, the terrain on the northeast side of the fault is a combination of bare soil and phreatophytes with scattered houses and patches of irrigated vegetation. The spectral properties of this soil regime produce the dark signature that contrasts with the regional light-colored signature of the barren, sand-mantled Coachella Valley.

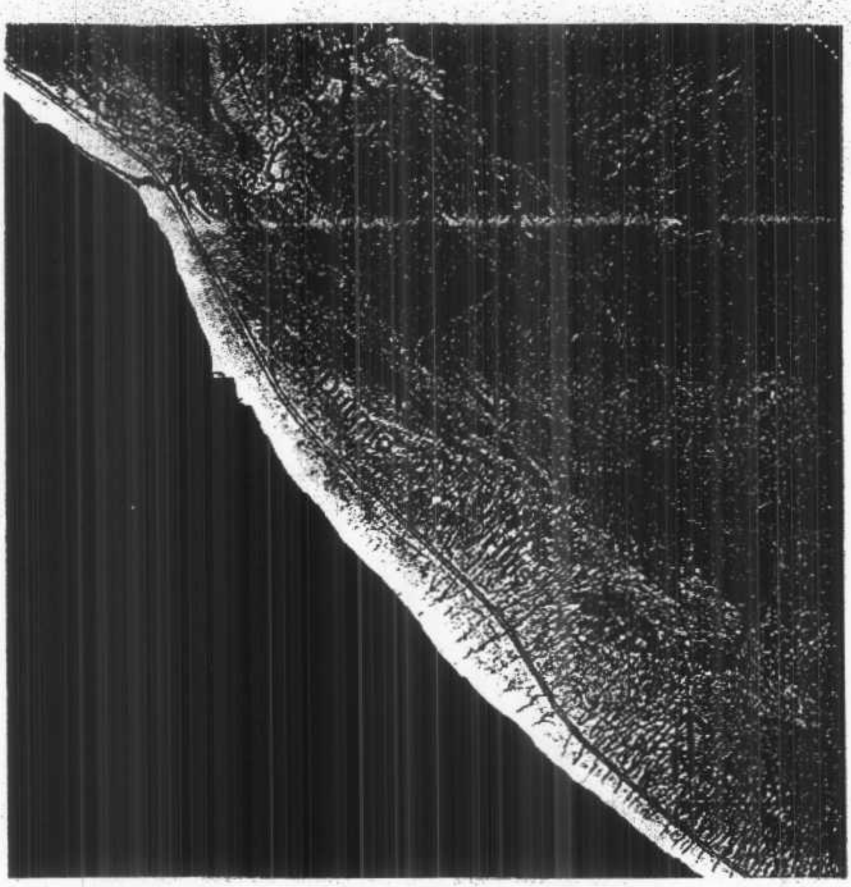

Figure 5. High-altitude aerial photograph of the Durmid Hills structural culmination along the San Andreas right-slip fault (dotted line), California. Deformation associated with this Neogene wrench fault consists of a system of east-trending folds arranged in an *en echelon* pattern and oblique to the San Andreas fault. Figure 6 is a photographic enlargement depicting some of these folds. Note the youthful drainage pattern associated with this uplift and indicative of regional dip. Also note the right-lateral offset of Salt Creek along the San Andreas fault.

Along the southeastern margin of the Indio Hills where the Banning fault merges with the Mission Creek fault to form the San Andreas fault, the merged faults cause several groundwater seeps that support small groves of native palms. These palm groves are readily detected on Landsat images at 1:100,000 scale. At the smaller scale of Figure 3, however, these groves are not detectable.

The northeastern margin of the southeastern Indio Hills is a northeast-facing, linear scarp framed by the Indio Hills fault. This fault is projected northward into the foothills of the Little San Bernardino Mountains. The Indio Hills fault has a distinctive linear topographic appearance on the Landsat image (see Figure 3).

There are a number a small anticlines and synclines in the Indio Hills that apparently formed in response to displacements along the Banning and Mission Creek right-slip faults. Most of the folds are only a few miles long with steeply dipping limbs that locally are overturned. The folds are most obvious in the well-bedded sandstone and siltstone of the Palm Spring formation. The folds are not recognizable on the images because of their small size and complex erosion patterns.

One recognizable fold is Edom Hill at the northwestern end of the Indio Hills (see Figure 3). The broad, doubly plunging anticline is four miles long and trends northwest, parallel with the Banning fault that cuts the flank of the fold. Edom Hill rises over a thousand feet above the desert floor, with its geomorphology controlled by the anticline. Radial drainage channels are beginning to erode the slopes of the hill which is underlain by poorly stratified Ocotillo Conglomerate. The domal shape, radial drainage, and local flatirons are keys in recognizing the anticline on the Landsat image. Many years ago, Texaco drilled an unsuccessful oil test on the crest of Edom Hill.

Mecca Hills

The Mecca Hills lie between Interstate 10 and Highway 111 in the southeastern part of the Coachella Valley just north of the Salton Sea (Figure 4). This wedge-shaped, northwest-trending topographic welt is a structural culmination along the San Andreas fault system, as are the Indio Hills to the northwest and the Durmid Hills to the southeast (Sylvester, 1988). The Mecca Hills offer one of best localities for viewing the complex folding and faulting that commonly occur along the San Andreas and other wrench-fault systems.

The stratigraphy of the Mecca Hills is similar to that of the Indio Hills with the addition of deeper exposures into the basement complex. Much of the gravel-covered frontal slopes of the Mecca Hills is underlain by poorly lithified, Pleistocene-age Ocotillo Conglomerate which contains schists detritus derived from the Orocopia Mountains to the east. On the southwestern margin of the hills, the conglomerate has been offset about 15 miles northwestward along the San Andreas fault since its deposition (Crowell and Sylvester, 1979). The higher, rugged parts of the Mecca Hills are composed of Plio-Pleistocene Palm Spring formation consisting of light-colored, well-indurated, arkosic sandstone and conglomerate.

These terrestrial sedimentary rocks grade southwestward and basinward into siltstone, and northeastward into alluvial-fan facies of the Canebrake Conglomerate.

In the core of the Mecca Hills, the lower part of the Palm Spring formation is interbedded and underlain by the Late Miocene(?)-Pliocene Mecca formation, a reddish to dark reddish-brown unit of thick-bedded sandstone, claystone, conglomerate, and breccia (Sylvester and Smith, 1976). The detrital material of these rocks is composed chiefly of Mesozoic and Precambrian basement debris. The Mecca formation, in turn, lies nonconformably on a heterogeneous basement complex of Precambrian gneiss, Mesozoic granitic rocks, and mid-Tertiary hypabyssal felsic dikes which, in the subsurface, is in thrust-fault contact over the late Mesozoic(?)-age Orocopia Schist. The young Cenozoic sedimentary section in the Mecca Hills is interrupted by numerous diastems and abrupt facies changes that reflect Pliocene-Pleistocene episodes of folding and faulting along the northeastern rim of the Salton trough.

The Mecca Hills uplift is bounded by the San Andreas fault on the southwest and the Hidden Springs fault on the northeast, and is cut longitudinally by the Painted Canyon and Eagle Canyon faults (see Figure 4). These faults form prominent canyons or valleys in the Mecca Hills or control right-slip offsets along major drainage courses. The more northerly Painted Canyon, Eagle Canyon, and Hidden Springs faults are normal-oblique, right-slip, horsetail-splay structures off the northwest-trending San Andreas fault. This fault-splay system is well expressed on the Landsat image as linear topographic features, and is characterisitic of a wrench-fault zone. The Plio-Pleistocene strata that make up much of the Mecca Hills exhibit complex faulting and folding associated with Neogene wrench-fault deformation. Strike-slip faults, normal oblique-slip and reverse oblique-slip faults, flower structures, inward-verging transpressive structures, and *en echelon* folds and faults are common structural elements within the Mecca Hills uplift. The details of these features are too small to be recognized on the Landsat image; however, major right-slip faults, large anticlinal culminations, and significant subsidiary faults are readily expressed on the remote sensing data.

Durmid Hills

The tectonic regime in the Durmid Hills is dominated by right-slip, wrench-fault transpression associated with the San Andreas fault (Figure 5). In these low hills, a sequence of layered, soft, lacustrine sedimentary rocks are deformed pervasively into a system of east-trending folds that are arranged in a right-stepping, *en echelon* pattern and oblique to the San Andreas fault (Figure 6). These folds are associated with wrench-fault deformation along the San Andreas fault, suggestive to the wrench-fault clay models as presented by Wilcox and others (1973).

The folds in the Durmid Hills are generally noncylindrical with thinned limbs and thickened hinges (i.e., *similar* style of folding; Burgmann, 1991). Their surface expression on the high-altitude aerial photographs consists of pronounced elliptical to elongate-elliptical outcrop patterns (see Figure 6). Wavelengths and amplitudes of the folds range from centimeters to hundreds of meters. As noted above, the folds at the Durmid Hills are arranged in an *en echelon* pattern, oblique to the San Andreas fault (see Figure 6). The mean trend of fold-axial traces is about N74°W, about 27° to the N47°W strike of the adjacent San Andreas fault (Burgmann, 1991). The angle between the fold-axial trace and the strike of the San Andreas fault commonly decreases toward the fault. That is, the folds trend toward parallelism with the San Andreas fault immediate to the fault (see Figure 6).

The present-day uplift of the Durmid Hills is shown by the youthful drainage pattern in the area, peaked by the San Andreas fault (see Figures 5 and 6). The Durmid Hills themselves, rising to a height of about 60 meters (200 feet), are geomorphic evidence for tectonic uplift. A leveling array over the uplift indicates that the Durmid Hills rose relative to the Salton Sea at a rate of about 1 mm/yr from 1985 to 1987 (Sylvester, 1988). The antecedent Salt Creek (see Figure 5) cuts about 40 meters (130 feet) into the uplifted Durmid Hills in the last 25,400 ± 2200 years, giving an uplift rate of about 1 to 2 mm/yr (Burgmann, 1991). Based on the exposed stratigraphy of the Pleistocene Borrego formation in the Durmid Hills, a total uplift of 200 to 1300 meters in 740,000 years (age of Bishop Ash) was estimated (Burgmann, 1991). This corresponds to uplift rates of 0.27 to 1.76 mm/yr over the last 740,000 years.

Right-lateral separation along the San Andreas fault is evident at Salt Creek where it has been offset by about 600 to 800 meters (see Figure 5). Vertical stratigraphic separation across the San Andreas fault has been measured at about 500 to 1120 meters with the northeast side relatively higher than the southwest side of the fault (Babcock, 1974). This vertical separation along the San Andreas fault in the Durmid Hills is associated with transpressive movement of the right-slip, wrench-fault zone.

The San Andreas right-slip fault appears to die at the southern end of the Durmid Hills. At this point, the fault system is believed to jog southwestward across the Imperial Valley to the right-lateral, normal-oblique slip Imperial fault (see Figure 1). The following discussion focuses on this right-stepping fault jog of the San Andreas fault system in the Imperial Valley.

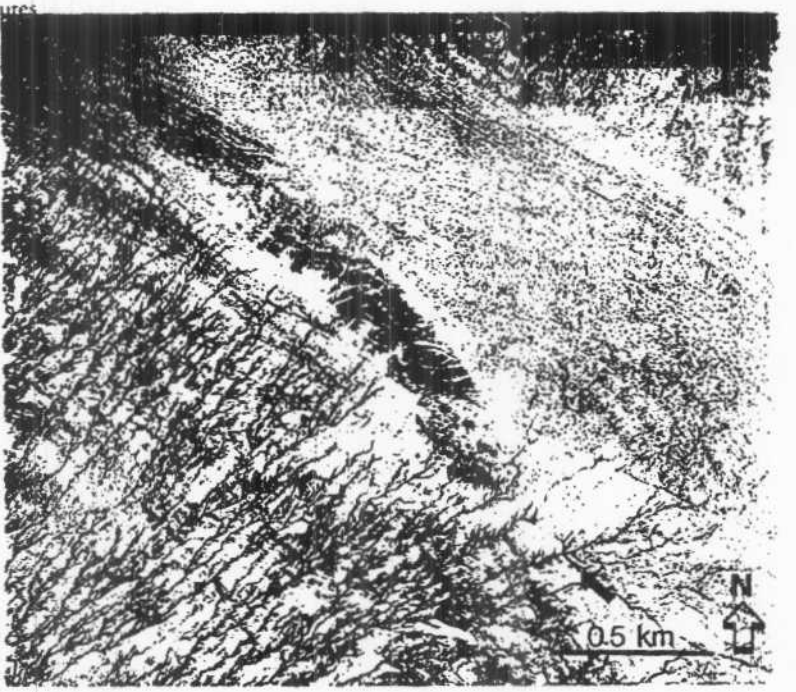

Figure 6. High-altitude aerial photograph of east-trending, right-stepping, *en echelon* folds on the northeast side of the San Andreas fault (arrows) in the Durmid Hills, California (see Figure 5 for location). Note the youthful drainage pattern that defines the recently uplifted, southwestern margin of the San Andreas fault.

Imperial Valley

The Imperial Valley of southern California represents the transition from the San Andreas transform-fault system on the northwest, to the Gulf of California right-transform system on the southeast. Neotectonics in the valley are indicative of right-slip transtension presumably associated with the San Andreas right-lateral, transform, wrench-fault system. The main strand of the San Andreas fault in this region is last exposed in the Durmid Hills along the southeastern margin of the Salton Sea (see Figure 1). From there, the fault system is believed to jog southeastward across the Imperial Valley through a system of northwest-trending, right-slip faults interconnected by transtensional basins (e.g., Hill, 1977; Elders, 1979; Sharp, 1982; Lachenbruch and others, 1985; Sibson, 1987; Lonsdale, 1989; Corona and others, 1991). The presence of active geothermal systems in the Imperial Valley and Salton trough results from the transtensional opening of the valley.

Structures in the Imperial Valley associated with the neotectonic activity along the San Andreas-Imperial fault system are obscured by the major agricultural development in the valley (Figure 7). However, the synoptic character of the Landsat Thematic Mapper data does reveal hints of the underlying structural geology. Linear features defined by straight stream segments and low-relief topographic scarps appear to correspond, in many cases, to known, subtly exposed, surface faults (e.g., Imperial fault), to buried extensions of well-defined surface faults (e.g., Superstition Hills and Superstition Mountain faults), or to postulated subsurface faults.

Three principal trends can be delineated on the satellite image in the Imperial Valley: northwest, north-south, and northeast (see Figure 7). Northwest-trending features are probably related to primary or secondary right-lateral, strike-slip faults; north-striking elements may be extensional or oblique-normal slip in nature; and northeast-trending structures are likely to be subsidiary, conjugate, left-slip faults. Actual slip sense of these features are difficult to determine from the Landsat data; however, field observations and published literature support the implied displacements.

Figure 7. Landsat Thematic Mapper image of the Imperial Valley area, California, with structures and linear features identifiable on the satellite data. Line weight (i.e., solid, dashed, and dotted) correspond to the level of expression of the mapped feature. Note that northwest-trending features are probably right-slip faults, north-striking elements may be extensional in nature, and northeast-trending structures are likely to be left-slip faults. **IF**, Imperial fault; **SHF**, Superstition Hills fault; **SMF**, Superstition Mountain fault.

Analysis and interpretation of potential field data in the Imperial Valley concur with a right-stepping, right-slip, fault-jog system (Corona and others, 1991). From these data, the tectonic framework of the Imperial Valley was interpreted to be dominated by northwest-trending, right-stepping, right-lateral strike-slip faults that are connected by a series of basins or basinal blocks and cut in places by northeast-trending left-slip structures. The basins appear to be bounded and segmented by north-trending structures that are oblique to the northwest-trending right-slip faults. These structures may be basin-forming faults or dike-injected fracture zones that are interpreted to be extensional in nature. This structural configuration is compatible with wrench-fault transtension.

SUMMARY AND CONCLUSIONS

In summary, wrench faults and their structural-style assemblage can be identified on remote sensing or surface geologic data with the following criteria:

- The principal fault or displacement zone is long and relatively straight to slightly curved.
- Major strike-slip fault zones commonly occupy valleys.
- Structural relief along major strike-slip faults is inconsistent in that structurally high areas alternate repeatedly across the faults.
- Splay, parallel, and conjugate faults may occur adjacent to or diverge from the principal wrench-fault zone, forming anastomosing or horsetail fault patterns.
- *En echelon* structures may develop on either side of the principal or secondary strike-slip fault zone, forming at an oblique angle to the zone.
- Lateral offset or bending of structural, natural, or man-made features may be visible across the fault.

- Transpression or transtension along a wrench-fault zone may be recognized by the dominance of contractional or extensional structures, respectively.

These criteria define distinguishing surface characteristics of wrench-fault assemblages that differentiate them from other styles of deformation. As shown in this examination, remote sensing data can be used in practical geologic interpretation of structures and structural styles. The approach is to determine the diagnostic geometric characteristics of individual structural elements, and avoid detailed identification and mapping of every linear and curvilinear feature on these data that may or may not be related to geologic structures. The type, orientation, and distribution of these elements are then mapped and analyzed to establish a structural style. With this approach, a better understanding of regional as well as individual structures in both well-mapped and frontier areas can be developed. Remote sensing data can present a complimentary view in regional geologic analysis.

REFERENCES CITED

Babcock, E. A., 1974. Geology of the northeast margin of the Salton trough, Salton Sea, California. Geol. Soc. America Bull., 85:321-332.

Burgmann, R., 1991. Transpression along the southern San Andreas fault, Durmid Hill, California. Tectonics, 10:1152-1163.

Christie-Blick, N., and K.T. Biddle, 1985. Deformation and basin formation along strike-slip faults, in K.T. Biddle and N. Christie-Blick, eds., Strike-slip deformation, basin formation, and sedimentation.Soc. Econ. Paleont. Miner., Spec. Publ. 37:1-34.

Corona, F. V., 1993. Recognition of wrench-fault systems, in F.V. Corona, F.F. Sabins Jr. and E.G. Frost, fieldtrip leaders, The San Andreas Fault System: Ninth Thematic Conf. Geologic Remote Sensing, Pasadena, California:32-63.

Corona, F. V., S.F. Krupicka, G.T. Ririe and E.A.E. Johnson, 1991. The structural framework of the Imperial Valley area, southeastern California, derived from Landsat and image-enhanced potential field data. San Diego, Geol. Soc. America, Abs. with Programs, 23(5):A91.

Corona, F. V., F.F. Sabins Jr., and E.G. Frost, fieldtrip leaders, 1993. The San Andreas Fault System. Ninth Thematic Conf. Geologic Remote Sensing, Pasadena, California: 210 p.

Crowell, J. C., 1962. Displacement along the San Andreas fault, California. Geol. Soc. America Spec. Paper, 71: 61 p.

Crowell, J. C., and A.G. Sylvester, eds., 1979. Tectonics of the junction between the San Andreas fault system and the Salton trough, southeastern California - a guidebook. Dept. of Geol. Sci., Univ. California Santa Barbara: 193 p.

Dibblee, T. W., Jr., 1977. Strike-slip tectonics of the San Andreas fault and its role in Cenozoic basin evolvement, in T.H. Nilsen, ed., Late Mesozoic and Cenozoic sedimentation and tectonics in California. Bakersfield, California, San Joaquin Geol. Soc:26-38.

Elders, W. A., 1979. The geological background of the geothermal fields of the Salton trough, in W.A. Elders, ed., Geology and geothermics of the Salton trough. Geol. Soc. America Guidebook, Fieldtrip No. 7:1-19.

Harding, T. P., 1974. Petroleum traps associated with wrench faults. Amer. Assoc. Petrol. Geologists Bull., 58:1290-1304.

___, 1990. Identification of wrench-faults using subsurface structural data: criteria and pitfalls. Amer. Assoc. Petrol. Geologists Bull., 74: 1590-1609.

Harding, T. P., and J.D. Lowell, 1979. Structural styles, their plate-tectonic habitats, and hydrocarbon traps in petroleum provinces. Amer. Assoc. Petrol. Geologists Bull., 63:1016-1058.

Lowell, J. D., 1990. Structural styles in petroleum exploration. Oil & Gas Consultants International Publications, Tulsa, Oklahoma, 3rd printing: 470 p.

Hill, D. P. 1977., A model for earthquake swarms. Jour. Geophys. Res., 82:1347-1352.

Hutton, L. K., L.M. Jones, E. Hauksson and D.D. Given, 1991. Seismotectonics of southern California, in D.B. Slemmons, E.R. Engdahl, M.D. Zoback and D.D. Blackwell, eds., Neotectonics of North America. Boulder, Colorado, Geol. Soc. America, Decade Map, 1:133-152.

Lachenbruch, A. H., J.H. Sass and S.P. Galanis Jr., 1985. Heat flow in southernmost California and the origin of the Salton trough. Jour. Geophys. Res., 90:6709-6736.

Lonsdale, P., 1989. Geology and tectonic history of the Gulf of California, in E.L. Winterer, D.M. Hussong and R.W. Decker, eds., The Eastern Pacific Ocean and Hawaii. Geol. Soc. America, The Geology of North America, N:499-521.

Reading, H. G., 1980. Characteristics and recognition of strike-slip fault systems, in P.F. Ballance, P. F. and H.G. Reading, Sedimentation in oblique-slip mobile zones. Intl. Assoc. Sediment., Spec. Pub, 4:7-26.

Sabins, F. F., 1967. Infrared imagery and geologic aspects. Photogrammetric Engineering, 29:83-87.

Sharp, R. V., 1982. Tectonic setting of the Imperial Valley region, in The Imperial Valley, California, earthquake of October 15, 1979. U.S. Geol. Survey Prof. Paper, 1254:5-14.

Sibson, R. H., 1987. Earthquake rupturing as a mineralizing agent in hydrothermal systems. Geology, 15:701-704.

Sylvester, A. G., 1988. Strike-slip faults. Geol. Soc. America Bull., 100:1666-1703.

Sylvester, A. G., and R.R. Smith, 1976. Tectonic transpression and basement-controlled deformation in San Andreas fault zone, Salton trough, California. Amer. Assoc. Petrol. Geologists Bull., 60:2081-2102.

Wilcox, R. E., T.P. Harding and D.R. Seely, 1973. Basic wrench tectonics. Amer. Assoc. Petrol. Geologists Bull., 57:74-96.